Journal of the Ceramic Society of Japan 121 [8] 611-613 2013 Paper

Morphology and surface structure of cubic $BaTiO_3$ using first-principles density functional theory

Masanobu NAKAYAMA,[*,,***,†] Shota HOTTA,[*] Tomoaki NAKAMURA[*] and Toshihiro KASUGA[****]**

[*]Department of Materials Science and Engineering, Nagoya Institute of Technology, Gokiso, Showa, Nagoya 466–8555, Japan
[**]Japan Science and Technology Agency, PRESTO, 4–1–8 Honcho Kawaguchi, Saitama 332–0012, Japan
[***]Unit of Elements Strategy Initiative for Catalysts & Batteries (ESICB), Kyoto University, Katsura, Saikyo-ku, Kyoto 615–8520, Japan
[****]Department of Frontier Materials, Nagoya Institute of Technology, Gokiso, Showa, Nagoya 466–8555, Japan

First-priciples density functional theory (DFT) techniques are used to provide atomic-scale insight into the surface structures and crystal morphologies of cubic barium titanate, $BaTiO_3$. Relaxed surface structures and energies are calculated for 3 low index planes and resulting equilibrium morphology based on Wulff's theorem with {001} and {011} faces were constructed. The calculated surface energies are strongly dependent on the coordination loss of TiO_6 octahedra at the surface. The optimized structure at the low-energy surfaces shows that only atoms at 1st perovskite layer are displaced from ideal position, while no significant displacements are indicated. On the other hand, the Bader charge analysis shows that the ionicity of whole the cations in the slab (7 perovskite layers) is larger than that in the bulk. Therefore, change of electric property is expected at the surface region, which is not due to the surface reconstruction, but to the change of electronic structure.

Key-words : First-principles DFT, Surface structure, $BaTiO_3$, Crystal morphology

[Received April 9, 2013; Accepted May 15, 2013]

1. Introduction

Perovskite-type $BaTiO_3$ (BT) particles used as raw materials for electronic devices, such as multilayered ceramic capacitors (MLCC), has attracted considerable attentions owning to their excellent dielectric properties, and the fundamental fascination of the relationship between their various electronic properties and crystal structure.[1)] Therefore, BT materials have been studied extensively for many years. One of the interesting phenomena related to BT materials is a "size effect", in which the ferroelectricity reduces with decreasing particle size and vanishes below certain critical size.[2)–8)] In addition, Wada et al. reported ultrahigh dielectric constants of ~15 000, when the particle size approaches to 60 nm.[8)] They found that the BT nano-particles possessed two regions of (a) a surface cubic and (b) a bulk tetragonal BT structures. This suggests observed high dielectric constants related to the surface cubic-BT structure, since the contribution of surface becomes emphasized by nanorization.

To clarify the effect of surface structure and energies of cubic-BT, first-principles density functional theory (DFT) has been performed in this paper. The thermodynamic equilibrium shape (morphology) of a crystal was determined through the Wulff construction procedure.[9)] The crystal and electronic structures are discussed for the sake of understanding electronic properties of particle size effect in the BT compound.

2. Methodology

All first-principles DFT calculations were performed using the Vienna ab initio simulation package (VASP)[10),11)] with the modified Perdew–Burke–Ernzerhof generalized gradient approximation (GGA-PBEsol)[12),13)] and projector-augmented wave (PAW) method.[14)] Spin polarization calculation was adopted. An energy cutoff was of 500 eV and appropriate k-point meshes are chosen to ensure that the total energies are converged within 3 meV per $BaTiO_3$. The relaxation of lattice parameters and fractional coordinates was allowed for the bulk cubic-BT structure, and the final energies of the optimized geometries were recalculated to correct for changes in the plane-wave basis during the relaxation, unless specifically mentioned otherwise.

The surface cubic-BT structures were simulated using the slab technique, in which a set of infinite layers separated by vacuum layers are repeated periodically along the surface normal.[15)] The slabs were constructed such that the two sides of it are symmetrically equivalent and can be mapped into each other by an inversion or mirror type of symmetry operation in the middle of the slab. Only three low-index facets of (001), (011), and (111) surfaces were calculated in present computations due to expensive computational cost for these surface simulations. In addition, charge-balanced stoichiometric slabs are only considered by adjusting the number of surface atoms keeping above symmetry constraint in this study. Total 6 termination models were constructed as follows; BaO- and TiO_2-terminated (001) surfaces, O_2- and BaTiO-terminated (011) surfaces, and Ti- and BaO_3-terminated surfaces. (See **Fig. 1**.) All the bulk and slab calculations were performed taking the symmetry into account during ionic relaxation, which prevents the transition to lower symmetric phase for the bulk and cancels polarity appeared at top and bottom of the slab.

3. Result and discussion

The cubic lattice parameter of the bulk cubic-BT phase is 3.98899Å, showing good agreement with experimental one (3.996 Å at 393 K).[16)] The obtained cubic lattice parameter was set and fixed for *ab*-plane of the slab (parallel to slab) for the slab simulation, and only ions were allowed to relax. The thickness of

† Corresponding author: M. Nakayama; E-mail: masanobu@nitech.ac.jp

DOI http://dx.doi.org/10.2109/jcersj2.121.611

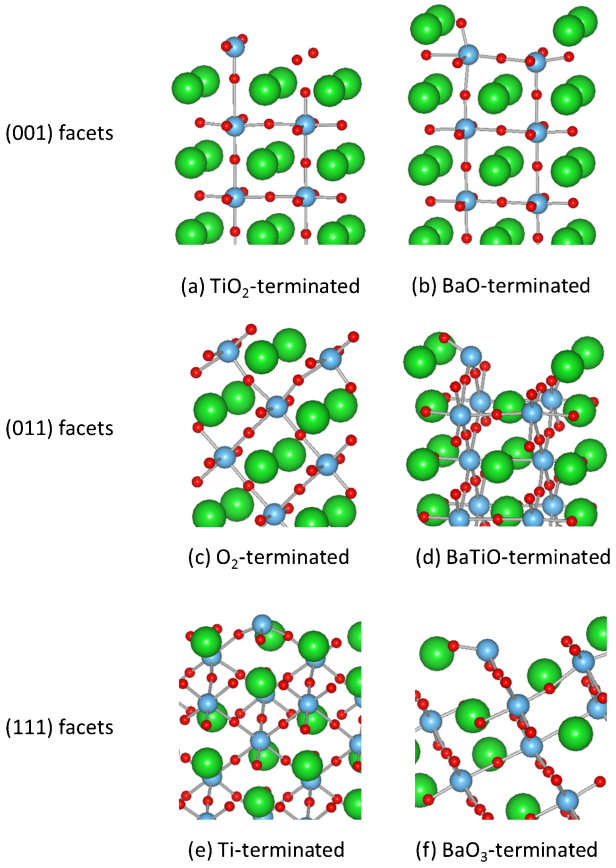

Fig. 1. Optimized surface structure of (001), (011), and (111) facets with two termination structure. The large, middle, and small spheres correspond to Ba, Ti, and O atoms, respectively, and Ti and O atoms are connected by bonds.

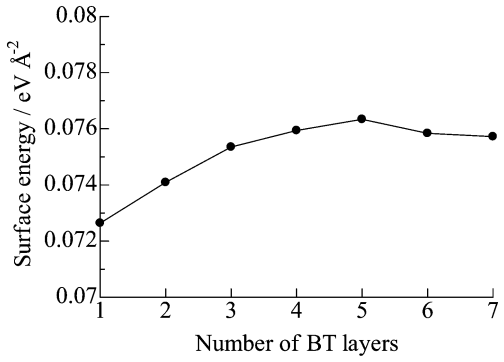

Fig. 2. Variation of the calculated surface energies with various slab thickness. The surface energy refers to the O_2-terminated (011) surface.

vacuum layer was set to be 10 Å in the present slab simulation. The surface energy, E_{surf}, can be determined for the stoichiometric slab simulation by following equation,

$$E_{surf} = 1/(n \cdot \sigma)[E_{slab}(Ba_nTi_nO_{3n}) - nE_{bulk}(BaTiO_3)]$$

in which E_{slab} and E_{bulk} refer to total energy of the slab and the bulk of cubic-BT, respectively, and n and σ stand for the mole number of BT phase and the surface area, respectively, in the corresponding slab model. **Figure 2** displays typical examples of calculated surface energies as a function of number of perovskite layers along c-axis, i.e. the thickness of cubic-BT slab. The surface energy converged if more than six cubic-BT layers are considered. Hence, the surface structures and energies refer to the model with the slab thickness of seven cubic-BT lattices, unless specially mentioned. We also calculated total energies for several surface configurations by increasing periodicity in parallel to slab layer, and minor change in energy (<0.5 meV Å^2) is indicated. **Table 1** lists the calculated surface energies for six slab models. Among six low-index orientations, (001) and (001) surfaces shows relatively small surface energies. We infer that the difference in the surface energy stems from coordination loss of TiO_6 octahedra. [The coordination loss stands for the difference of coordination number of Ti between at surface (i-fold) and at bulk (sixfold Ti).] As seen in Fig. 1, the number of coordination loss of TiO_6 octahedra at surface is unity, i.e. fivefold Ti, for stable BaO-terminated (001) and O_2-terminated (011) surfaces. On the other hand, threefold Ti ions can be seen for unstable TiO_2-terminated (001) surface, and so on. This agrees with former first-principles DFT study on $LiFePO_4$ material, in which the coordination loss at the transition metal, Fe, causes surface energies increase largely.[17]

Table 1. Surface energies of cubic $BaTiO_3$ in three low-index directions with two sets of termination. (See main text)

Surfaces	(001)		(011)		(111)	
Termination*	BaO	TiO_2	O_2	BaTiO	Ti	BaO_3
γ /eV Å^{-2}	0.076	0.263	0.072	0.107	0.104	0.100

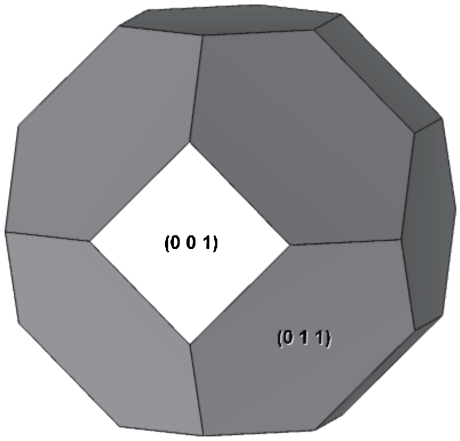

Fig. 3. Wulff shape of $BaTiO_3$ using calculated surface energies at Table 1.

The crystal morphology at equilibrium was predicted from the surface energies to be minimal for a given volume. This can be determined based on Wulff's theorem, in which the distance to the central point {hkl} from the origin is taken to be proportional to the surface energy.[9),17)–19)] **Figure 3** presents the calculated crystal morphology at equilibrium (Wulff shape). The facets of (111) were not appeared in the present computation due to relatively high surface energies. The surface area of (011) facets are almost 4 times as large as that of (001) facets. The calculated morphology in Fig. 1 agrees with the former computational results for $LaCoO_3$.[18)] Note that the surface energies and Wulff shape were calculated based on the vacuum | cubic-BT interface. Hence, a variety of the crystal morphologies was conceivable, depending on synthesis condition, such as atmosphere. Hereinafter in this report, we focus on the reconstructed structures of BaO-terminated (001) and O_2 terminated-(011) surfaces. **Table 2** show the interatomic distances between Ba and Ba, and Ti and Ti perpendicular to the slab layer, where both the ideal distance are the same as the cubic lattice parameter. (3.988 Å) The displacement of the atoms by surface reconstruction is indicated at the first layer, so that the cubic symmetry was broken. The Ba–Ba or Ti–Ti

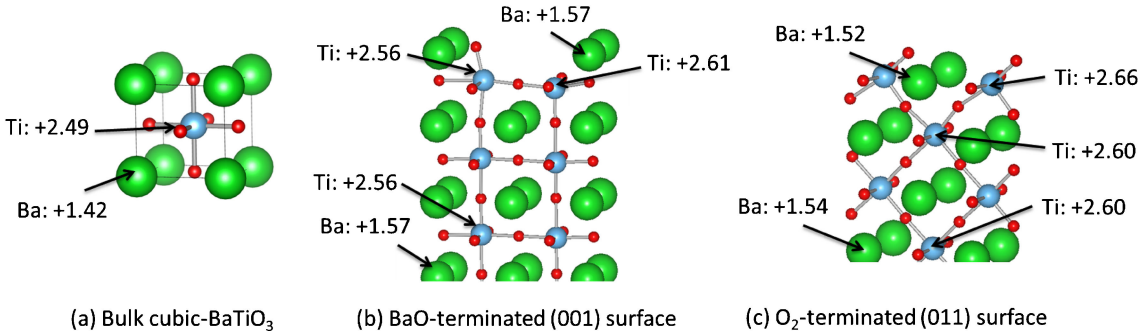

Fig. 4. Bader charges of selected cations in (a) the bulk, (c) BaO-terminated (001), and (c) O_2-terminated (011) facets of cubic-BT phase.

Table 2. Interatomic distances of Ba–Ba and Ti–Ti perpendicular to the slab layer

	BaO-terminated (001) surface		O_2-terminated (011) surface	
	Ba–Ba/Å	Ti–Ti/Å	Ba–Ba/Å	Ti–Ti/Å
1st layer	3.856	4.147	4.087	3.857
2nd layer	4.029	4.033	3.991	4.054
3rd layer	4.012	4.013	4.029	3.953

interatomic distances at (001) or (011) surfaces were reduced from ideal lattice parameter, while Ti–Ti interatomic distance at the (011) surface was increased. On the other hand, the interatomic distances at 2nd and 3rd layers were almost the same with ideal lattice parameter or tended to increase slightly. Therefore, the effect of the structural reconstruction may only appear at the top several perovskite layers in cubic-BT phase. In order to analyze electronic structure, a grid based Bader charge analysis was performed for Ba and Ti ions in the bulk, and the (001) and (011) surfaces (**Fig. 4**). Bader charge is the integrated charge density inside a zero flux surface in which the charge density is a minimum perpendicular to the surface.[20)–23)] The Bader charges of Ba and Ti atoms are around +1.5 and +2.5, respectively. The obtained cation charges were smaller than nominal charges, which may associate with the contribution of covalent bonding nature and/or the intuitive criteria of Bader's theory. According to the Pauling's suggestion,[24)] the iconicity of the Ba–O and Ti–O bonds are 80% (+1.6) and 60% (+2.4), respectively, showing rough accordance with Bader's charges. The Bader's charges of Ba and Ti in the (001) and (011) slab models are larger than those in the bulk structure. Hence, the iconicity of the ions in the surface regions is relatively higher than that in the bulk. In addition, no large difference was seen in the charges between the top and interior of the slab models. Slight larger charges for the top fivefold Ti atoms may stem from the criteria of Bader's theory rather than the change of ionicity. This suggests the difference between the surface and the bulk electronic structure does not owe to the structural reconstruction by displacement of the ions from the ideal position, but to the local potential difference.

In summary, present paper discussed the surface energy and morphology of cubic-BT phase. The surface energy is strongly related to the coordination loss of the Ti ions, and the relatively higher iconicity is indicated at the surface than at the bulk of cubic-BT phase. Further study on surface dielectric properties and potential analyses is required.

Acknowledgement The present work was partially supported by JST PRESTO program, Grant-in-Aid for Scientific Research (No. 257959) from MEXT, and "Elements Strategy Initiative to Form Core Research Center" (Since 2012) from MEXT, (MEXT; Ministry of Education Culture, Sports, Science and Technology, Japan). Figures of the crystal structure were drawn with VESTA.[25)]

References

1) P. P. Phule and S. H. Risbud, *J. Mater. Sci.*, 25, 1169–1183 (1990).
2) K. Kinoshita and A. Yamaji, *J. Appl. Phys.*, 47, 371–373 (1976).
3) G. Arlt, D. Hennings and G. De With, *J. Appl. Phys.*, 58, 1619–1625 (1985).
4) K. Ishikawa, K. Yoshikawa and N. Okada, *J. Am. Ceram. Soc.*, 72, 1555–1558 (1989).
5) S. Wada, T. Suzuki and T. Noma, *Jpn. J. Appl. Phys.*, 34, 5368–5379 (1995).
6) M. H. Frey and D. A. Payne, *Phys. Rev. B*, 37, 3158–3168 (1996).
7) S. Wada, T. Suzuki and T. Noma, *J. Ceram. Soc. Japan*, 104, 383–392 (1996).
8) S. Wada, T. Hoshina, K. Takazawa, M. Ohsishi, H. Yasuno, H. Kakemoto and T. Tsurumi, *J. Korean Phys. Soc.*, 51, 878–881 (2007).
9) G. Wulff, *Z. Kristallogr. Mineral.*, 34, 449–530 (1901).
10) G. Kresse and J. Furthmuller, *Phys. Rev. B*, 54, 11169–11186 (1996).
11) G. Kresse and J. Furthmuller, *Comput. Mater. Sci.*, 6, 15–50 (1996).
12) J. P. Perdew, K. Burke and M. Ernzerhof, *Phys. Rev. Lett.*, 77, 3865–3868 (1996).
13) J. P. Perdew, A. Ruzsinszky, G. I. Csonka, O. A. Vydrov, G. E. Scuseria, L. A. Constantin, X. Zhou and K. Burke, *Phys. Rev. Lett.*, 100, 136406 (2008).
14) P. E. Blöchl, *Phys. Rev. B*, 50, 17953–17979 (1994).
15) A. Christensen and E. A. Carter, *Phys. Rev. B*, 58, 8050–8064 (1998).
16) S. Miyake and R. Ueda, *J. Phys. Soc. Jpn.*, 2, 93–97 (1947).
17) L. Wang, F. Zhou, Y. S. Meng and G. Ceder, *Phys. Rev. B*, 76, 165435 (2007).
18) M. S. D. Read, M. S. Islam, G. W. Watson, F. Kingc and F. E. Hancock, *J. Mater. Chem.*, 10, 2298–2305 (2000).
19) C. A. J. Fisher and M. S. Islam, *J. Mater. Chem.*, 18, 1209–1215 (2008).
20) R. F. W. Bader, "Atoms in Molecules-A Quantum Theory", Clarendon Press, Oxford, U.K. (1990).
21) G. Henkelman, A. Arnaldsson and H. Jónsson, *Comput. Mater. Sci.*, 36, 254–360 (2006).
22) E. Sanville, S. D. Kenny, R. Smith and G. Henkelman, *J. Comput. Chem.*, 28, 899–908 (2007).
23) W. Tang, E. Sanville and G. Henkelman, *J. Phys.: Condens. Matter*, 21, 084204 (2009).
24) L. Pauling, "The Nature of Chemical Bond" Cornell University Press, New York (1960).
25) K. Momma and F. Izumi, *J. Appl. Cryst.*, 41, 653–658 (2008).